Two-Stage Swelling of Acrylamide Gels: A Photon Transmission Study

ÖNDER PEKCAN,[1] SELIM KARA[2]

[1] Department of Physics, Istanbul Technical University, Maslak 80626, Istanbul, Turkey

[2] Department of Physics, Trakya University, Edirne 22030, Turkey

Received 15 May 2000; accepted 18 November 2000

ABSTRACT: Acrylamide gels were prepared from acrylamide (AAm) with various *N,N′*-methylenebis(acrylamide) (Bis) contents by free-radical crosslinking copolymerization (FCC) in water and dried before used for swelling experiments. Photon transmission measurements were performed using a UV-visible (UVV) spectrometer during the swelling of polyacrylamide gels. Transmitted light intensity I_{tr} increased linearly at very early times when acrylamide gels were immersed in water, then decreased continuously as swelling time increased. The behavior of I_{tr} was modeled assuming two-stage swelling mechanisms for the swelling acrylamide gels. The increase in I_{tr} at early times was quantified using a linear diffusion model and a linear relaxation constant k_0 was measured. The decrease in I_{tr} was modeled using the Li–Tanaka equation, from which time constants τ_1 and cooperative diffusion coefficients D_0 were determined for acrylamide gels with varying Bis content. © 2001 John Wiley & Sons, Inc. J Appl Polym Sci 82: 894–906, 2001

INTRODUCTION

It has been known that the swelling and elastic properties of gels are strongly influenced by large-scale heterogeneities in the network structure.[1,2] In the swollen state these imperfections manifest themselves in a nonuniformity of polymer concentration. These large-scale concentration heterogeneities do not appear during the gelation but only in the gel swollen at equilibrium.[3] Light-scattering experiments by Bastide et al.[4] seem to confirm this observation. The structural heterogeneities of a gel greatly affect its physical properties such as permeability, elasticity, and optical properties. It was shown that high permeability of acrylamide gels is related to the inhomogeneous crosslink distribution.[5,6] The effects of inhomogeneities of the polymer network on the swelling equilibrium of acrylamide gels and on the diffusion of water molecules within the gels were examined.[7] The network structure and its inhomogeneities can be varied by changing the concentration of polymers and the proportion of crosslinkers to polymers. A model that relates gel composition with the swelling ratio, turbidity, elastic modulus, and volume fraction was described for polyacrylamide gels.[8] The boundary between a transparent state and an opaque, heterogeneous state for a gel as a function of monomer and crosslinker concentrations was determined.[9]

Swelling is directly related to the viscoelastic properties of a gel. The gel elasticity and the friction between the network and solvent play an important role on the kinetics of the gel swelling.[10–12] It has been known that the relaxation time of swelling is proportional to the square of a linear size of the gel,[10] which has been confirmed

Correspondence to: Ö. Pekcan.

Journal of Applied Polymer Science, Vol. 82, 894–906 (2001)

experimentally.[12] One of the most important features of the gel swelling process is that it is isotropic. The elastic and swelling properties of permanent networks can be understood by considering two opposing effects, the osmotic pressure and the restraining force. Usually the total free energy of a chemically crosslinked network can be separated into two terms: the bulk and the shear energies. In a swollen network the characteristic quantity of the bulk free energy is the osmotic bulk modulus K. The other important energy, the shear energy, keeps the gel in shape by minimizing the nonisotropic deformation. The characteristic coefficient of these forces is the shear modulus μ, which can be most directly evaluated by stress–strain measurements.[1,13] Li and Tanaka[14] developed a model in which the shear modulus plays an important role that keeps the gel in shape as a result of coupling of any change in different directions. This model predicts that the geometry of the gel is an important factor and that swelling is not a pure diffusion process.

The equilibrium swelling and shrinking processes of polyacrylamide gels in solvent have been extensively studied[15–17.] It has been reported that acrylamide gels undergo continuous or discontinuous volume phase transitions with temperature, solvent composition, pH, and ionic composition.[15] pH-induced volume transitions of acrylamide gels in an acetone/water mixture were studied using fluorescence technique. When an ionized acrylamide gel is allowed to swell in water, an extremely interesting pattern appears on the surface of the gel and the volume expansion increases by adding some amount of sodium acrylate.[17] If acrylamide gels are swollen in an acetone/water mixture, gel aging time plays an important role during collapse of the network.[17] The kinetics of swelling of acrylamide gels was studied by light scattering and the cooperative diffusion coefficient of the network was measured.[10,18] Small-angle X-ray and dynamic light scattering were used to study the swelling properties and mechanical behavior of acrylamide gels.[19,20] An *in situ* photon transmission technique, used to study aging of acrylamide gels attributed to multiple swelling, was reported from our laboratory,[21] where it was observed that the transmitted light intensity I_{tr} decreases continuously as acrylamide gel swells. The decrease in I_{tr} was attributed to the structural inhomogeneities in the gel.[22–24]

In this work *in situ* photon transmission experiments were reported during the swelling of acryl-

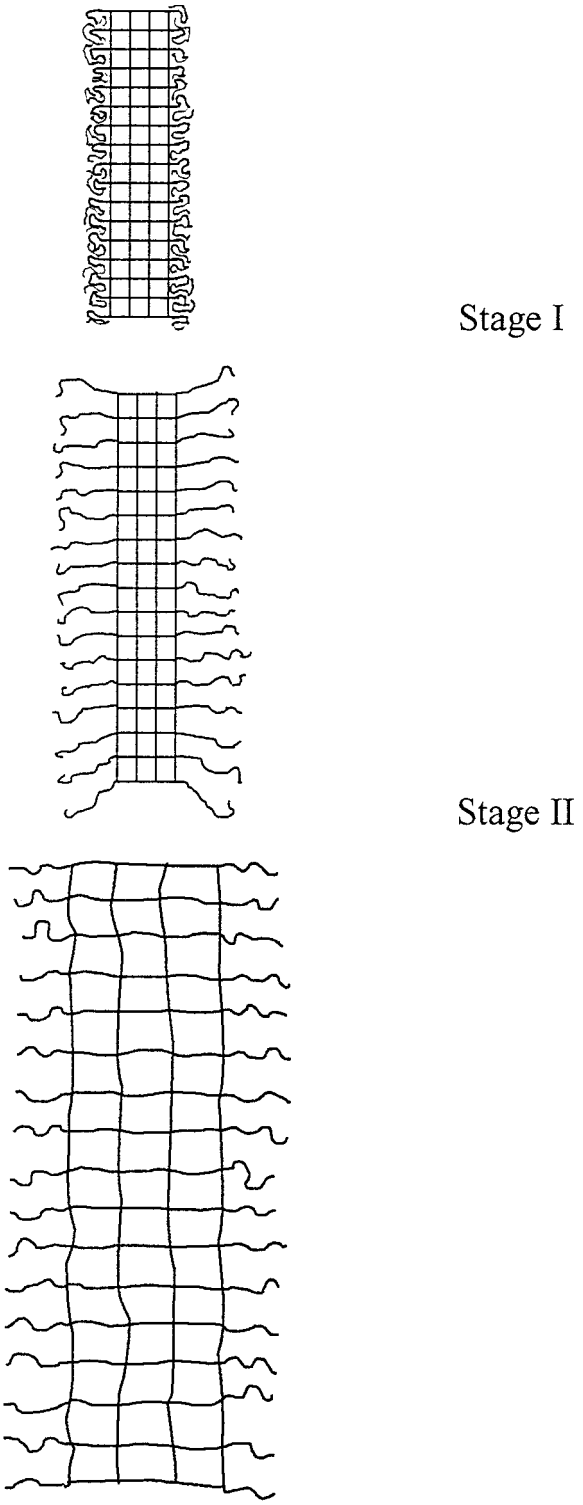

Figure 1 Schematic representation of two-stage gel swelling. Stage I presents linear diffusion at the surface of the gel. Stage II describes the Li–Tanaka model at the center of the gel.

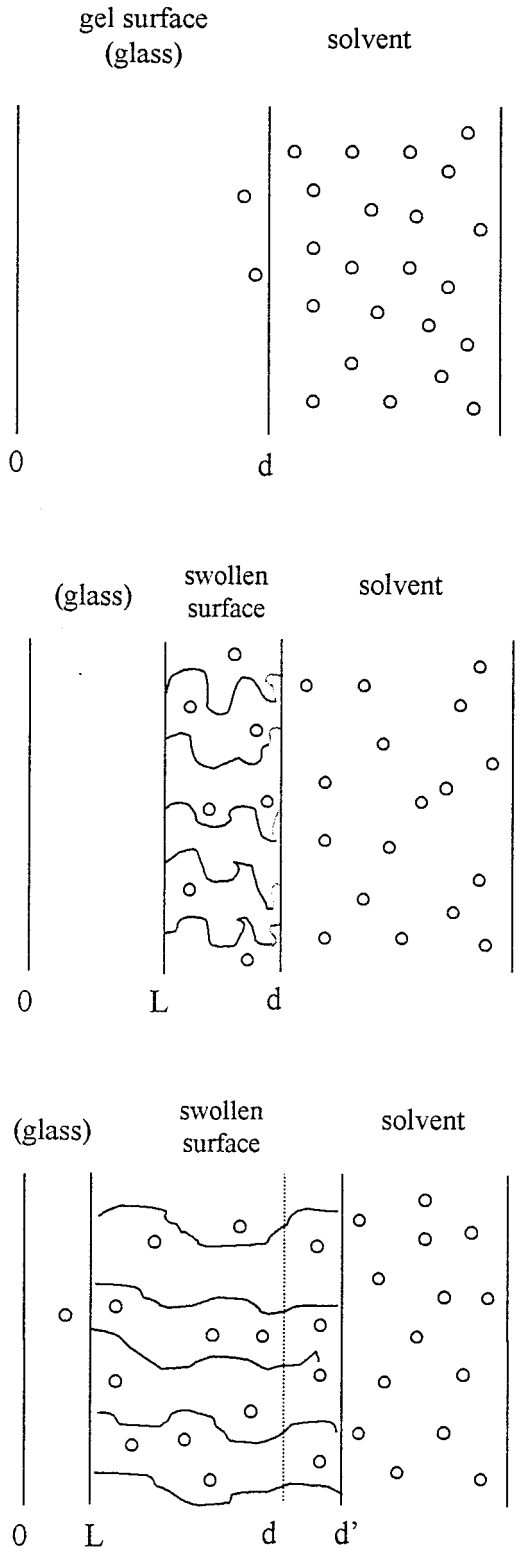

Figure 2 A schematic presentation of swelling at the surface of the gel.

amide gels prepared with various Bis contents. It was observed that the transmitted light intensities I_{tr} at early times increased suddenly and then decreased exponentially as the gels swelled. The increase in I_{tr} was attributed to the surface swelling of the gel, which was modeled using a linear diffusion process. The decrease in I_{tr} was attributed to the increase in scattered light intensity I_{sc} from the gel resulting from spatial heterogeneities, which increase during swelling of the center of the gel. The decrease in I_{tr} against time was modeled using the Li–Tanaka equation.[14] Time constants τ_1 and cooperative diffusion coefficients D_0 were determined for each gel sample with different Bis contents. I_{tr} intensities were measured by a UV-visible (UVV) spectrometric technique and swelling in acrylamide gels was monitored in real time by using the time-drive mode of the UVV spectrometer. Supporting experiments were performed by measuring the thickness and the weight of the gels during swelling processes.

KINETICS OF TWO-STAGE SWELLING

It is well known that for a macroscopic size gel, the swelling of the portion near the gel surface may be different compared with that in the center of the gel. This difference certainly complicates the kinetic studies; therefore, here we propose two different mechanisms in different time intervals for the gel swelling: (1) "linear diffusion," which takes place at early times of swelling and deals with the swelling near the gel surfaces; and (2) the Li–Tanaka model explains the swelling of the gel at the center, which takes place at longer times. These two stages of swelling are schematically presented in Figure 1.

Linear Diffusion Model

The linear transport mechanism is characterized by the following steps.[25] As the solvent molecules start to enter through the surface of the gel, an advancing boundary forms and separates the glassy part of the gel from the swollen surface (see Fig. 2). This boundary moves into the center of the gel at a constant velocity. The swollen gel behind the advancing front is always at a uniform state of swelling. Now consider a cross section of a surface with thickness d, undergoing linear diffusion as in Figure 2, where L is the position of the advancing sorption front, C_0 is the equilibrium penetrant concentration, and k_0 (mg cm^{-2} min^{-1})

is defined as the linear relaxation constant. The kinetic expression for the sorption in the surface gel slab of an area A is given by

$$\frac{dW}{dt} = k_0 A \tag{1}$$

The amount of solvent W absorbed in time t will be

$$W = C_0 A(d' - L) \tag{2}$$

where d' is the value of d at time t. After eq. (2) is substituted into eq. (1) the following relation is obtained:

$$\frac{d}{dt}(d' - L) = -\frac{k_0}{C_0} \tag{3}$$

By integrating eq. (3) one can obtain the following relation:

$$L = d' - \frac{k_0}{C_0} t \tag{4}$$

Here it is assumed that cross section A stayed constant during swelling, at least seen by UV beam. Given that $W = k_0 At$ and $W_m = C_0 Ad$, the following relation is obtained:

$$\frac{W}{W_m} = \frac{k_0}{C_0 d} t \tag{5}$$

where W_m is the maximum solvent sorption by the gel surface.

Li–Tanaka Model

The total energy of a gel can be separated into a bulk energy and shear energy. The bulk energy is related to the volume change, which is controlled by the following diffusion equation:

$$\frac{\partial \vec{u}}{\partial t} = D_0 \vec{\nabla}^2 \vec{u} \tag{6}$$

where $\vec{u}$ is the displacement vector of a point in the network and D_0 is the collective diffusion coefficient. The shear energy F_{sh}, on the other hand, can be minimized instantly by readjusting the shape of the gel; that is, the change of the shear energy in response to any small change in shape that maintains constant volume element within the gel should be zero.[14]

$$\delta F_{sh} = 0 \tag{7}$$

Simultaneous solution of eqs. (6) and (7) produces the following equation for the swelling of a gel disk[14]:

$$\frac{u(r, t)}{u(r, o)} = \sum_n B_n \exp(-t/\tau_n) \tag{8}$$

where the displacement vector is expressed as a decomposition into components, each of them decaying exponentially with a time constant τ_n. The first term of the expression is dominant at large t, that is, at the last stage of swelling. Equation (8) can also be written in terms of solvent uptakes W and W_∞ at time t and at equilibrium, respectively, as follows[26]:

$$\frac{W_\infty - W}{W_\infty} = \sum_{n=1}^{\infty} B_n \exp(-t/\tau_n) \tag{9}$$

In the limit of large t or if τ_1 is much greater than the rest of τ_n, all higher terms ($n \geq 2$) in eq. (9) can be omitted, so that the swelling kinetic can be given by the following relation:

$$\left(1 - \frac{W}{W_\infty}\right) = B_1 \exp(-t/\tau_1) \tag{10}$$

Here B_1 is related to the ratio of the shear modulus μ and the longitudinal osmotic modulus $M = [K + (4\mu/3)]$. Once the value of B_1 is obtained, one can determine the value of $R = \mu/M$ because the dependence of B_1 and R for a disk can be found in the literature.[14] τ_1 is related to the collective cooperative diffusion coefficient D_0 of a gel disk as

$$D_0 = \frac{3a_\infty}{\tau_1 \alpha_1^2} \tag{11}$$

where α_1 is a function of R only (given in the literature[11]) and a_∞ is the half thickness of the gel in the final equilibrium state. Once the quantities τ_1 and B_1 are obtained, R, α_1, and D_0 can be calculated.

TURBIDITY OF GELS

A gel can be described as a random distribution of crosslinks on a lattice formed by the interchain contact points. When two junctions are located on neighboring lattice sites, a "frozen blob" is formed.[4] In the swollen state of a gel these crosslinks cannot move apart from each other because they are chemically connected by a chain segment, which is in an optimal excluded volume conformation. Frozen blobs are often connected and form clusters of first topological neighbors. As a result the random crosslinking of chains can be described as a site percolation on a blob lattice. When the gel is in a good solvent it swells and frozen blob clusters expand less than the interstitial medium.

When the gel is in a swollen state small clusters are expelled from larger ones, creating regions of low concentration. Here the correlation length becomes the typical size of clusters that are not entangled with smaller ones. In other words, correlation length becomes the typical size of holes that are created as a part of the interstitial medium. Here the swelling of gel leads to an excess scattering of light, which comes from the contrast between frozen blob clusters and holes created by the dilution. During the dilution process in gel swelling, the partial separation of frozen blob clusters leads to a strong increase of the scattering intensity I_{sc} or decrease in the transmitted light intensity I_{tr}, which is the case when the central part of the gel swells. However, when the surface of the gel swells, dangling ends relax by creating more homogeneous lattice for I_{tr}, with the result that it increases during surface swelling.

EXPERIMENTAL

Gels were prepared by using 2.5 g of AAm and 40 mg of ammonium persulfate (APS) as an initiator by dissolving them in 25 cc of water in which 10 μL of tetramethyl ethylenediamine was added as an accelerator. Four different gels were obtained by adding 175, 200, 250, and 300 mg Bis into each of the gels prepared by the above procedure. Free-radical crosslinking copolymerization was performed at room temperature in a 1.6-cm diameter cylindrical cell in nitrogen atmosphere. Disc-shape gels were obtained by cutting these cylindrical gels; 1.4- to 1.6-mm-thick gels in various Bis contents were placed into a 1 $\times$ 1-cm quartz cell filled with water for the UVV experiments. Swelling of gel discs was monitored in real time and *in situ* photon transmission measurements were performed using a Perkin–Elmer UVV spectrometer (Perkin Elmer Cetus, Norwalk, CT).

Typical normalized I_{tr} curves against swelling time t_s are given in Figure 3 for the experiments made at 550 nm wavelength for four different Bis content samples. In Figure 3 it is seen that I_{tr} intensities increased suddenly at early times by reaching the highest transparency, then decreased exponentially, presenting the appearance of turbidity in these gel samples. The early-time behavior of I_{tr} was most probably caused by the surface imperfections of the gel, which may appear during the cutting process. The sudden increase of I_{tr} can be labeled as the surface effect related to the dangling chain ends, which relax during solvent sorption by presenting temporary transparency. This effect disappears at later times of swelling after I_{tr} reaches the maxima. Further swelling predicts that 175, 200, 250, and 300 mg Bis content gels present lattice heterogeneities, which increase as a result of the swelling process by causing a decrease in I_{tr}. Supporting experiments by measuring the thickness, radii, and the weight of the gels were performed using calipers, optical microscope, and a digital balance, during and after the swelling processes.

Variations of the thickness and the radii of the gel samples are plotted versus swelling time t_s, in Figure 4(a) and (b), respectively. In Figure 4(a) it is seen that gel thickness increases suddenly to twice its initial value, after which it levels off and continues to increase slowly to reach its final equilibrium. Here the early-time increase in thickness most probably comes from the swelling of gel at the surface, which is quite linear in time. However, the slow increase in thickness at later times comes from the swelling of gel at the center, which also presents quite linear behavior. On the other hand, the increase in radius of gel, presented in Figure 4(b), shows exponential behavior, thus indicating that an increase in radius obeys a law that is different from that for an increase in thickness.

Figure 5(a) presents the variation of weight of the gels in time. Volume ($V = l\pi r^2$) of the gels during swelling is calculated from the data in Figure 4 and plotted in Figure 5(b) for comparison. In Figure 5 it is seen that both weight and volume of gels obey a similar swelling law, which is different from the law obeyed by the thickness of the gel.

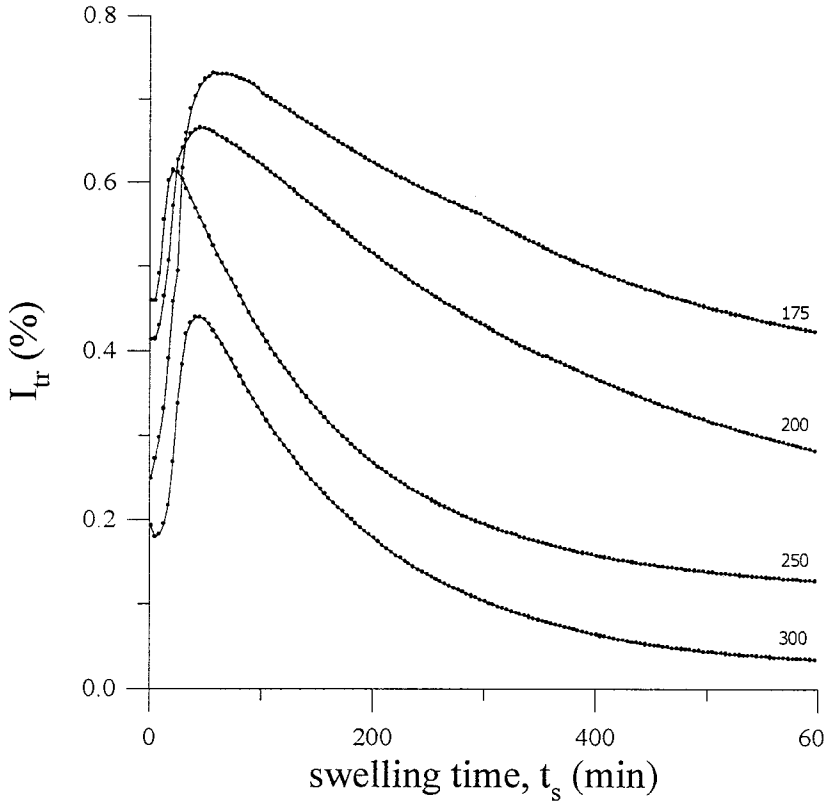

Figure 3 Plot of the I_{tr} curves versus swelling time at 550 nm wavelength. Numbers on each curve present Bis contents in mg.

RESULTS AND DISCUSSION

Swelling at the Surface

The short-time behavior of I_{tr} data versus t_s was plotted in Figure 6(a) for the gels with 175, 200, 250, and 300 mg Bis content, where quite linear relations were observed for all gel samples. To quantify these data, I_{tr} is assumed to be proportional to the solvent uptake W at the surface. This assumption can be realized by considering that some surface cracks disappear by absorption of water and, as a result, gel becomes quite transparent at early times. These cracks most probably originate from the dangling ends that appeared during the cutting of disc-shape gels from the cylindrical gel. Early absorption at the surface of the gels removes these inhomogeneities while the centers of the gels are still glassy and quite transparent. Equation (5) can be employed using the preceding argument, which becomes

$$\frac{I_{tr}}{I_0} = \frac{k_0}{C_0 d}\, t \tag{12}$$

where I_0 is the maximum of I_{tr} at the final surface swelling position. Fitting the data in Figure 3(a) at early times to eq. (12) produced k_0 values, listed in Table I, where C_0 = 600 mg/ml and d = 0.1 mm were taken. Results are shown in Figure 6(a). Here the loss of the light at the center of the gel is omitted.

Similar fittings were also made to the data in Figure 4(a) at early times. The results are given in Figure 6(b), where k_0' values were produced (listed in Table I), which are in accord with the previous values obtained from the I_{tr} data. Here it is assumed that the thickness of the center of the gel ($2a_\infty$) does not change during surface swelling, and the following equation is obeyed:

$$\frac{l}{l_0} = \frac{k_0'}{C_0 d}\, t \tag{13}$$

Here $l = d + a_\infty$, where a_∞ is the half thickness of the center of the gel and l_0 is the maximum value of the gel thickness l.

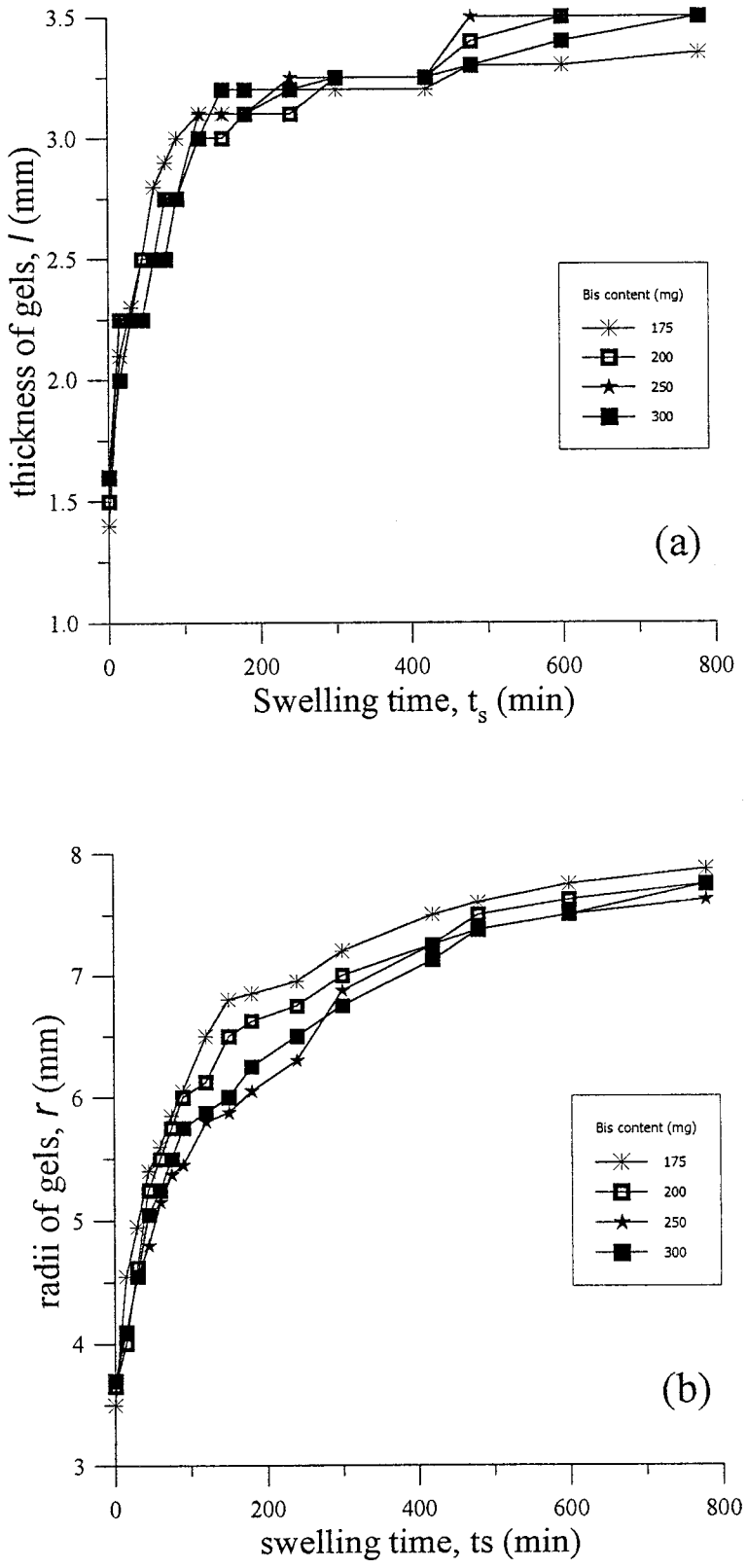

Figure 4 Variation of (a) thickness l and (b) radii r of the gel samples versus swelling time t_s.

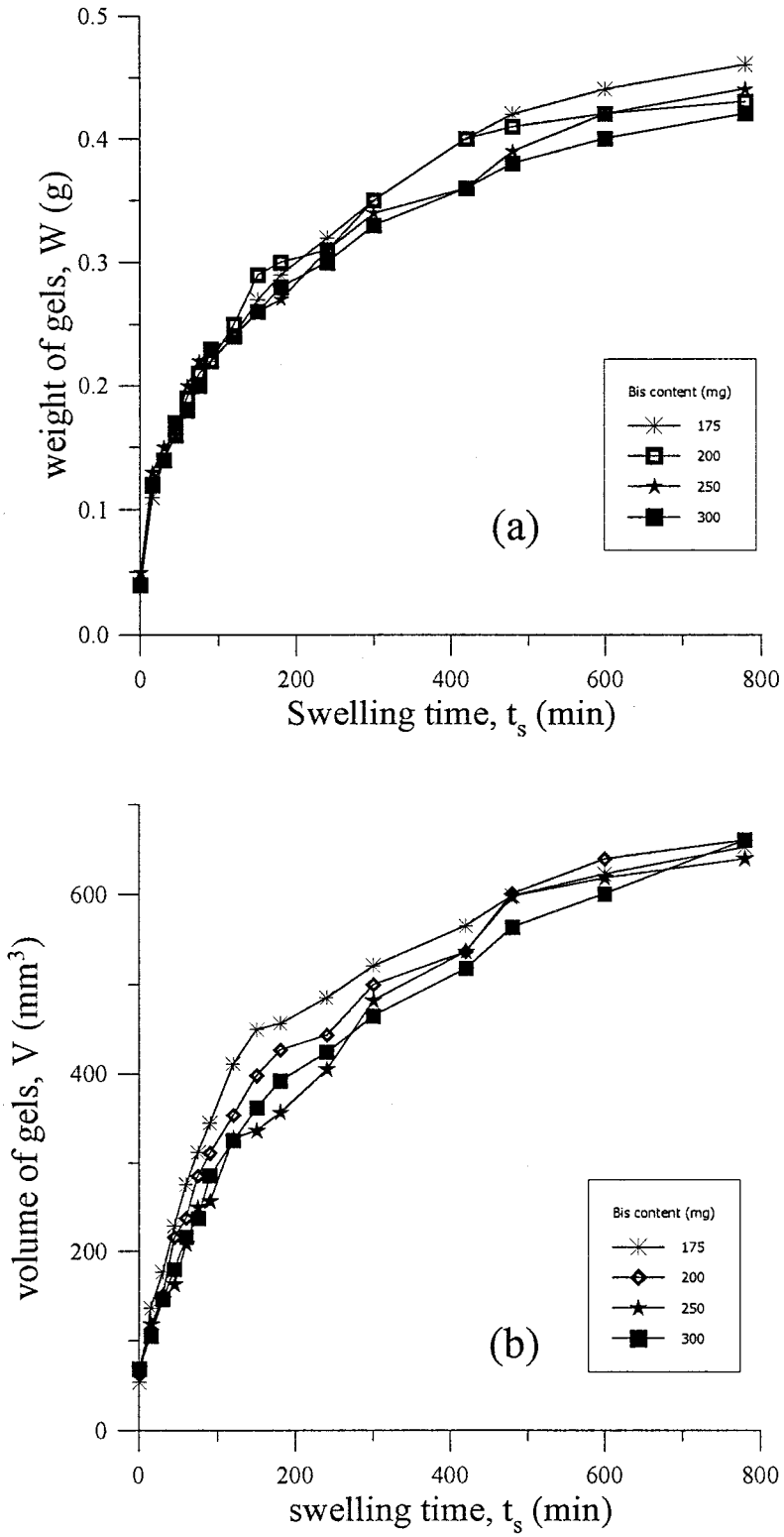

Figure 5 Variation of (a) weight W and (b) volume V of gels versus swelling time t_s.

Swelling at the Center

The behavior of I_{tr} above the maxima in Figure 3 can be quantified by establishing the relation between eq. (10) and I_{tr}. At the maxima, before solvent penetration starts to the center of the gel, the transmitted light intensity is given by I_0. Af-

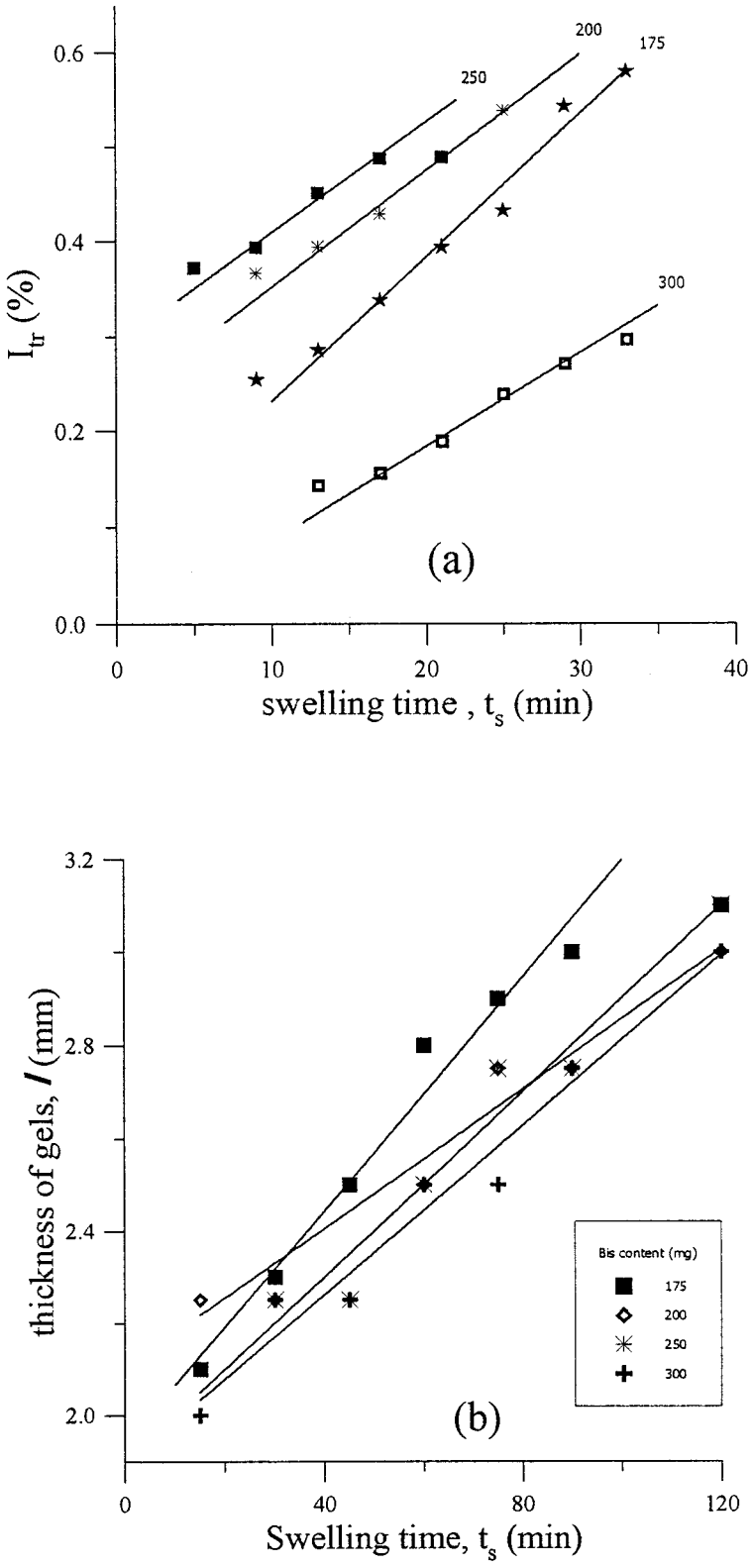

Figure 6 Short-time behavior of (a) I_{tr} and (b) thickness l versus swelling time t_s. The fits of the data to eqs. (12) and (13) are also presented, respectively.

Table I Viscoelastic and Swelling Properties of Acrylamide Gels with Varying Bis Contents[a]

	Bis Content (mg)			
	175	200	250	300
k_0 (I_{tr}) ($\times 10^{-3}$ mg cm^{-2} min^{-1})	89	74	70	59
k'_0 (l) ($\times 10^{-3}$ mg cm^{-2} min^{-1})	78	52	61	54
B_1	0.79	0.73	0.68	0.56
τ_1 (min)	864	583	214	177
D_0 ($\times 10^{-8}$ cm^2/s)	60	73	182	175
B'_1	0.79	0.78	0.74	0.75
τ'_1 (min)	239	205	249	230
D'_0 ($\times 10^{-8}$ cm^2/s)	209	258	190	217
B''_1	0.87	0.88	0.86	0.88
τ''_1 (min)	152	188	249	221
D''_0 ($\times 10^{-8}$ cm^2/s)	429	482	314	409

[a] Relaxation constants k_0 and k'_0 were obtained from eqs. (12) and (13). B_1 and τ_1 values were determined using eq. (16). B'_1, τ'_1 and B''_1, τ''_1 were obtained from eqs. (10) and (17), respectively. D_0, D'_0, and D''_0 values were determined using eq. (11).

ter the solvent molecules arrive at the center of the gel, attributed to the turbidity created by frozen blob clusters, transmitted intensity decreases to I_{tr} at time t_s, where the amount of solvent uptake is W. At the equilibrium state of swelling, the transmitted light intensity decreases to I_∞, where the solvent uptake by swollen gel is W_∞. The relation between solvent uptake W and transmitted intensities from the gel during the swelling process is expressed by the following:

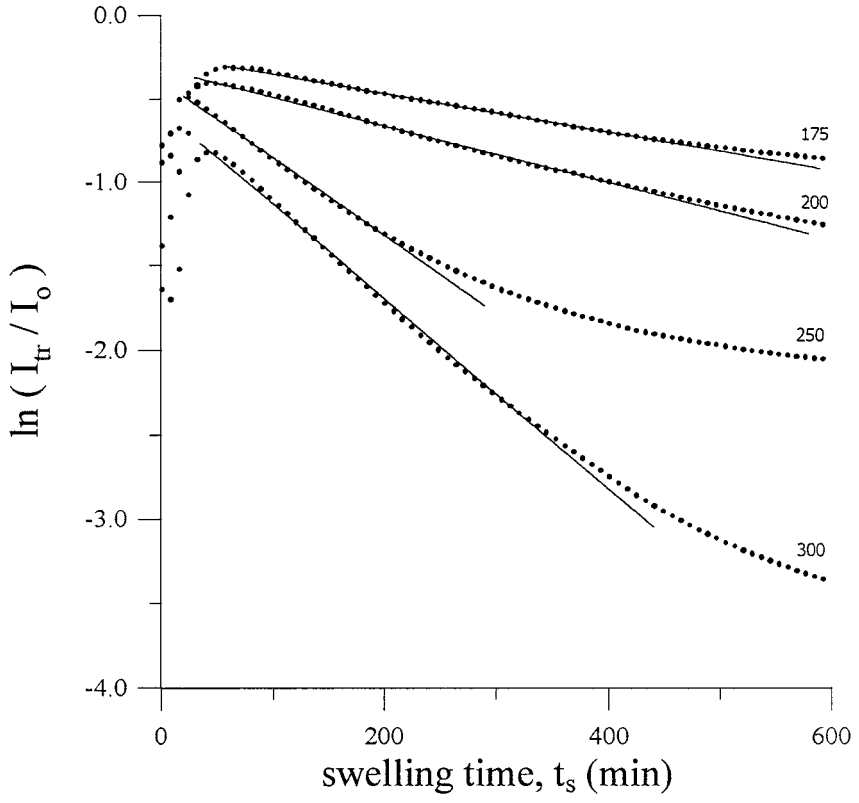

Figure 7 Plot of the data below maxima in Figure 3 according to eq. (16) at 550 nm wavelength. Numbers on each curve present the Bis content in mg.

$$\frac{W}{W_\infty} = \frac{I_0 - I_{tr}}{I_0 - I_\infty} \tag{14}$$

Given that $I_0 \gg I_\infty$, eq. (14) becomes

$$\frac{W}{W_\infty} = 1 - \frac{I_{tr}}{I_0} \tag{15}$$

This relation predicts that as W increases, I_{tr} decreases. By combining eqs. (15) and (10) and taking its logarithm the following relation can be obtained:

$$\ln(I_{tr}/I_0) = \ln B_1 - \frac{t_s}{\tau_1} \tag{16}$$

The data in Figure 3 below maxima are plotted in Figure 7 according to eq. (16), where quite linear relations are obtained. Linear regression of curves in Figure 7 provides us with B_1 and τ_1 values from eq. (16). Taking into account the dependence of B_1 and R, one obtains R values, and from $\alpha_1 - R$ dependence α values were produced.[14] Then using eq. (11), cooperative diffusion coefficients D_0 were determined for the center of gel samples, the results of which are listed in Table I. The measured time constant τ_1 and cooperative diffusion coefficients D_0 are plotted versus Bis content in Figure 8(a) and (b), respectively. It is seen in Figure 8(a) that τ_1 values exponentially decrease as the Bis content is increased, which indicates that swelling of loosely formed gels takes longer than swelling of densely formed gels. As a result D_0 values are smaller in loosely formed gels than in densely formed gels. The behaviors of these gels can be understood by realizing that loosely formed gels are more flexible and shear energy is much less in these gels than that in densely formed gels. As the crosslinker density of the gels increases, elastic contribution to the shear energy increases; as a result D_0 values increase, which is the case in densely formed gels.

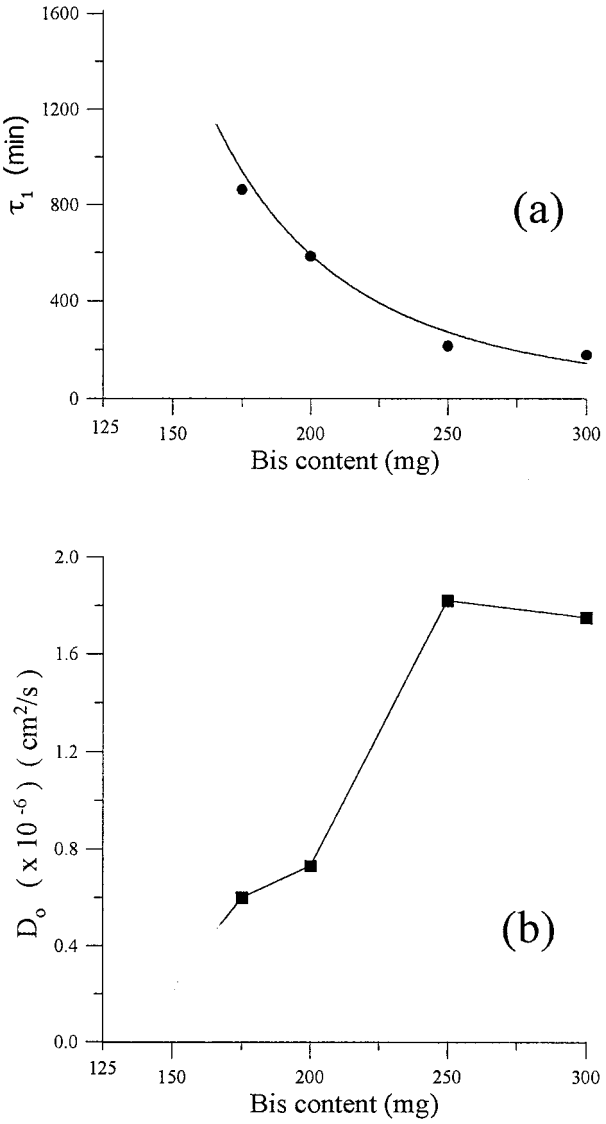

Figure 8 The plots of (a) τ_1 and (b) D_0 values versus Bis content for 550 nm wavelength.

Total Swelling

The data in Figure 5(a) are seen to be directly related to eq. (10), where W can be taken as the weight of the gels. The fit of the data in Figure 5(a) to eq. (10) is presented in Figure 9(a), from which linear regression produces B_1' and τ_1' values, which are listed in Table I. Using a similar treatment as that in the previous section, cooperative diffusion coefficients D_0' values were determined and are also listed in Table I.

The increase in the volume of gels, presented in Figure 5(b), also seems to obey the law in eq. (10), which can be written as

$$\left(1 - \frac{V}{V_\infty}\right) = B_1'' \exp(-t/\tau_1'') \tag{17}$$

where $V = l\pi r^2$ and V_∞ is the volume of the gel at the equilibrium state of swelling. The fit of the data in Figure 5(a) to eq. (17) produces the B_1'', τ_1'', and D_0'' values, which are given in Table I. From Table I it is seen that total swelling parameters

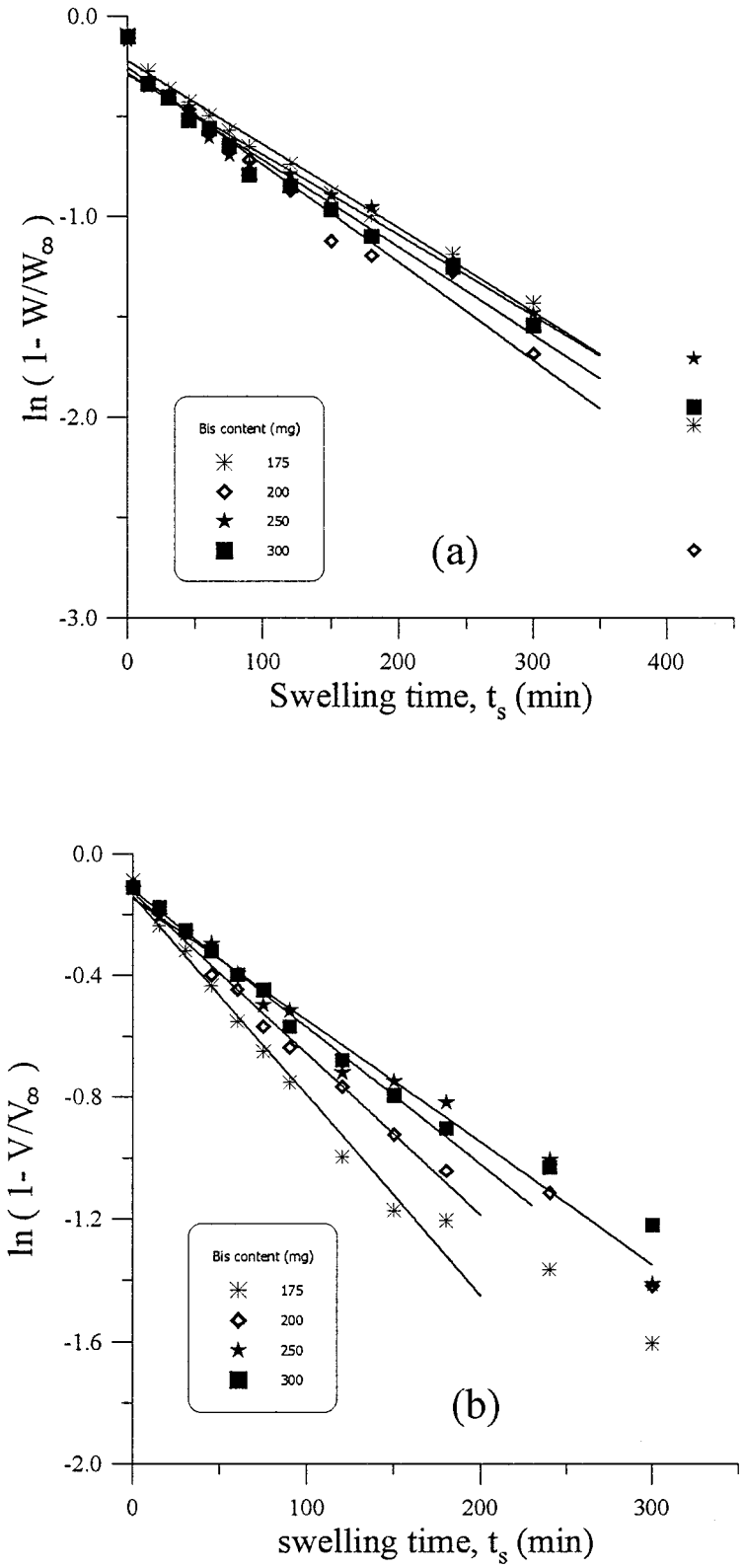

Figure 9 Fits of the data in Figure 5(a) and (b) to eqs. (10) and (17), respectively, are presented in (a) and (b).

τ_1', D_0' and τ_1'', D_0'', obtained from weight and volume increases of the gels during swellings, are all independent of Bis content. However, using the transmitted light technique, the observed parameters τ_1 and D_0 showed strong dependence on Bis content. Here we conclude that macroscopic techniques such as weighing out and volume measurements are not sensitive enough to determine the differences in solvent uptake by densely and loosely formed gels. However, the UVV technique is very sensitive to these kinds of measurements and its use is strongly suggested.

Here we also have to state that increases in thickness and radius during swelling of a disc-shape gel obey linear and pure diffusion models, respectively. By pure diffusion it is meant that Fickian diffusion is obeyed for radius swelling during the Li–Tanaka solvent uptake model. On the other hand, both volume and weight of the gel increase during swelling according to the Li–Tanaka equation.

REFERENCES

1. Dusek, K.; Prins, W. Adv Polym Sci 1969, 6, 1.
2. Silberger, A. Biological and Synthetic Networks; Kramer, O., Ed.; Elsevier: Amsterdam, 1988.
3. Bastide, J.; Leibler, L. Macromolecules 1988, 21, 2649.
4. Bastide, J.; Bove, F.; Busier, M. Molecular Basis of Polymer Networks; Baumgartner, A.; Picot, C., Eds.; Springer Verlag: Berlin, 1989.
5. Weiss, N.; Silberger, A. Polym Prepr (Am Chem Soc Div Polym Chem) 1975, 16, 289.
6. Weiss, N.; van Vliet, T.; Silberger, A. J Polym Sci Polym Phys Ed 1974, 17, 2229.
7. Hsu, T. P.; Ma, D. S.; Cohen, C. Polymer 1983, 24, 1273.
8. Richards, E. G.; Temple, J. C. Nat Phys Sci 1971, 230, 92.
9. Suzuki, Y.; Nozaki, K.; Yamamoto, T.; Itoh, K.; Nishio, I. J Chem Phys 1992, 97, 3808.
10. Tanaka, T.; Filmore, D. J Chem Phys 1979, 70, 1214.
11. Peters, A.; Candau, S. J. Macromolecules 1986, 19, 1952.
12. Chiarelli, P.; De Rossi, D. Prog Colloid Polym Sci 1988, 78, 4.
13. Candau, S. J.; Bastide, J.; Delsanti, M. Adv Polym Sci 1982, 7, 44.
14. Li, Y.; Tanaka, T. J Chem Phys 1990, 92, 1365.
15. Hirokawa, Y.; Tanaka, T. J Chem Phys 1984, 81, 6379.
16. Hu, Y.; Horie, K.; Ushiki, H. Macromolecules 1992, 25, 6040.
17. Tanaka, T.; Sun, S. T.; Hirokawa, Y.; Katayama, S.; Kucera, J.; Hirose, Y.; Amiya, T. Nature 1987, 325, 796.
18. Peters, A.; Candau, S. J. Macromolecules 1988, 21, 2278.
19. Ilavsky, M. Macromolecules 1982, 15, 782.
20. Patel, S. K.; Rodriguez, F.; Cohen, C. Polymer 1989, 30, 2198.
21. Pekcan, Ö.; Çatalgil–Giz, H.; Çalıskan, M. Polymer 1998, 39, 4453.
22. Kara, S.; Pekcan, Ö. Polym Compos 2000, 41, 3093.
23. Kara, S.; Pekcan, Ö. Polymer to appear.
24. Kara, S.; Pekcan, Ö. J Appl Polym Sci to appear.
25. Enscore, D. J.; Hopfenbergard, H. B.; Stannett, V. T. Polymer 1977, 18, 7931.
26. Wu, C.; Yang, C. Y. Macromolecules 1994, 27, 4516.